Location of the Head-Tail Junction of Myosin

David L. Rimm, John H. Sinard, and Thomas D. Pollard

Department of Cell Biology and Anatomy, Johns Hopkins School of Medicine, Baltimore, Maryland 21205

Abstract. The tails of double-headed myosin molecules consist of an alpha-helical/coiled-coil structure composed of two identical polypeptides with a heptad repeat of hydrophobic amino acids that starts immediately after a conserved proline near position 847. Both muscle and nonmuscle myosins have this heptad repeat and it has been assumed that proline 847 is physically located at the head-tail junction. We present two lines of evidence that this assumption is incorrect. First, we localized the binding sites of several monoclonal antibodies on *Acanthamoeba* myosin-II both physically, by electron microscopy, and chemically, with a series of truncated myosin-II peptides produced in bacteria. These data indicate that the head-tail junction is located near residue 900. Second, we compared the lengths of two truncated recombinant myosin-II tails with native myosin-II. The distances from the NH_2 termini to the tips of these short tails confirms the rise per residue (0.148 nm/residue) and establishes that the 86-nm tail of myosin-II must start near residue 900. We propose that the first 53 residues of heptad repeat of *Acanthamoeba* myosin-II and other myosins are located in the heads and the proteolytic separation of S-1 from rod occurs within the heads.

LIKE other proteins, myosin has been divided into domains by regions of protease sensitivity. Lowey et al. (1969) used papain to divide myosin into head and rod regions and trypsin to divide it into heavy meromyosin and light meromyosin. These proteolytic fragments have been used to correlate structure with function. The actin-binding site and the ATPase activity are located in the head region while the light meromyosin region of the rod is responsible for self assembly of bipolar filaments.

When the primary structure of several myosins was obtained by protein or DNA sequencing (Elzinga and Collins, 1977; Karn et al., 1983; Strehler et al., 1986; Warrick et al., 1986; Hammer et al., 1987) the boundaries between these functional domains appeared to be obvious. In every case the heads had a conserved sequence pattern with 40–90% identical residues even between protozoa and mammals (McLachlan and Karn, 1982; Emerson and Bernstein, 1987; Warrick and Spudich, 1987). This homology stops abruptly at a conserved proline located around position 840–850 that marks the beginning of a heptad repeat of hydrophobic residues. Thus, although the actual sequences of the tails differ in every case, this common pattern is present and indicative of the well-established alpha-helical/coiled-coil structure of the myosin tail. Consequently, it is universally assumed that the head-tail junction is at this conserved proline.

Myosin-II from *Acanthamoeba castellanii* has this characteristic heptad repeat (Hammer et al., 1987) beginning after proline 847 and ending at residue 1482 near the COOH terminus at 1509. This stretch of 635 amino acids has been assumed to form the alpha-helical/coiled-coil tail. Given a rise of 0.148 nm/residue in an alpha-helix (Fraser and Macrae, 1973; McLachlan, 1984), the sequence predicts that the tail should be 94 nm long. On the other hand, the length of the tail measured by electron microscopy is 86 nm (see Table I). Most other myosins have tails longer than 140 nm, so such a ~8-nm discrepancy could easily be dismissed as experimental error. In the case of *Acanthamoeba* myosin-II the discrepancy is particularly evident since, of all the double headed myosins, it has the shortest tail.

To investigate this discrepancy, we have used a set of recombinant fusion proteins expressed in bacteria to establish the relationship between the tail length measured by electron microscopy and the number of amino acids as well as to localize the chemical binding sites for several monoclonal antibodies to specific regions of amino acid sequence. We then compared these sequence locations with the physical location of the antibody binding sites that were established by electron microscopy. All of the data is consistent with the conclusion that the proximal seven to eight heptad repeats are included in the head placing the head-tail junction near residue 900.

Materials and Methods

Isolation of Acanthamoeba RNA

RNA was isolated from *Acanthamoeba* in mid-log phase by a modification of the method of Hammer et al. (1984). A 5-ml pellet of packed cells was added to 45 ml of a guanidine thiocyanate extraction buffer, vortexed, and then homogenized for 3.5 min in an omnimixer (Sorvall Instruments Div., Newton, CT). The homogenate was cooled on ice and centrifuged at 5,000 *g* for 10 min at 4°C. The supernatant was decanted and 100 μl of 2.5 M sodium acetate (pH 5.2) and 38 ml of ethanol were added. After precipitation at −20°C overnight, crude RNA was pelleted at 4,000 *g* for 15 min. The pellets were resuspended in 20 ml of 10 mM Tris-HCl (pH 7.5), 1 mM EDTA, 1% Sarkosyl, and 0.25 mg/ml proteinase K (Bethesda Research

Laboratories, Gaithersburg, MD) and incubated at 37°C for 40 min. The sample was extracted five times using a 2:1 mix of phenol/choroform (prepared as described in Maniatis et al., 1982). At each step the aqueous phase was transferred to a fresh tube. After two extractions with chloroform alone, the RNA was precipitated with ethanol in the presence of 0.25 M sodium acetate. The resulting RNA pellet was dried and resuspended in deionized water and stored at 5–10 mg/ml at −70°C until used. Northern analysis of the resulting RNAs showed that the 5 kb myosin-II message was intact and that there was very little degraded RNA (data not shown).

Construction and Screening of cDNA Libraries and Subcloning for Expression

Acanthamoeba RNA was used to produce a cDNA library in λgt10 essentially as described by Huynh et al. (1985). A poly-T primer was used with AMV reverse transcriptase (Life Sciences, Orlando, FL) to produce first strand. Second strand was produced with RNase H and Klenow fragment of DNA polymerase (Pharmacia Fine Chemicals, Piscataway, NJ) and the ends were blunted with S1 nuclease (Sigma Chemical Co., St. Louis, MO) and filled in with polymerase. Then phosphorylated Eco RI linkers (Collaborative Research, Lexington, MA) were ligated to the ends and cut with Eco RI (Promega Biotec, Madison, WI) to generate sticky ends. The cDNA was size fractionated and separated from free linkers on a 0.7 × 8 cm column of Biogel A1.5m (Bio-Rad Laboratories, Richmond, CA) and precipitated. We then ligated fractions containing different sizes of cDNA into prepared dephosphorylated Eco RI cut λgt10 arms (Stratagene, La Jolla, CA) and packaged the phage using Gigapack extracts (Stratagene). The resulting libraries had complexities of 1.0–6.5 × 10^5.

A library made from cDNAs >2,000 bp long was screened using a Pst I to Sal I fragment from the proximal tail region of the myosin-II genomic DNA provided by Dr. John Hammer III (National Institutes of Health, Bethesda, MD). Fig. 1 shows the restriction maps of a subset of our myosin-II clones that were used to localize the monoclonal antibody chemical binding sites.

Clones 3.6.1 and 3.8.1 and their engineered derivatives were expressed as fusion proteins in pUCX vectors (provided by P. Machlin and D. Cleveland, Johns Hopkins School of Medicine, Baltimore, MD). These vectors were produced from the pUC series of plasmid vectors and produce fusion proteins consisting of the first 12 amino acids of beta-galactosidase followed by residues coded by the cDNA. Clones 3.8.2, 3.8.2a, and 3.8.2b were expressed as fusions with 37 kD of the TrpE protein in the pATH-1 vector. Clones 3.9.3 and 3.12.2 were expressed in pATH 11. Clone N881 is a construct made by splicing the 5′ end of clone 3.12.2 with the 3′ end of 3.9.3 at an internal Aat II site. This clone and 3.9.3 were cloned into plasmid expression vector pRX-1 (Rimm and Pollard, 1989) to maximize the production of a fusion protein with only 18 residues of *Escherichia coli* TrpE protein. The resulting fusion proteins are called N881 and N942, respectively, for the first NH_2-terminal amino acids from myosin-II that are included in the fusion.

Production of Recombinant Proteins

The pUCX fusion proteins were produced by growing the plasmids in *E. coli* strain HB101 in RB medium (1.5% casamino acids, 0.5% tryptone, 0.5% yeast extract, 0.5% NaCl, 1% casein hydrolsate [ICN Biomedicals Inc., Irvine, CA] pH 7.5) for 3 h then inducing with 10 mM isopropyl-thiogalactosidase (Sigma Chemical Co., St. Louis, MO) and growing four more hours. The cells were harvested and washed once in 10 mM Tris-HCl, pH 8, then boiled in 1× sample buffer (Laemmli, 1970). The pATH and pRX fusion proteins were grown and harvested in the same manner except they were grown in M9-CA minimal medium (Maniatis et al., 1982) and induced with indoyl acrylic acid (Sigma Chemical Co.). To maximize expression for production of fusion proteins, *E. coli* strain CAG-456 (Baker et al., 1984) was used. Fusion proteins N881 and N942 were purified from 50 ml cultures by lysis in a buffer with lysozyme and Triton X-100 followed by ammonium sulfate fractionation, sizing, and ion exchange chromatography.

Localization of Chemical Binding Sites of Monoclonal Antibodies

Fusions proteins were run on SDS-PAGE (Laemmli, 1970) and blotted onto nitrocellulose (Towbin et al., 1979). The filter was blocked with 0.1% BSA in Tween buffer (10 mM Tris-HCl, pH 7.5, 150 mM NaCl, 0.5% Tween, and 1 mM thimerosal) then incubated with culture medium containing monoclonal antibody M2.46 for 1 h (see Kiehart et al., 1984*a*,*b*,*c* for description of antibody production and incubation). Peroxidase-linked goat anti-rabbit second antibody (HyClone Laboratories, Logan, UT) was added after three washes in Tween buffer. After a 1-h incubation and two Tween buffer washes the blot was washed twice with TBS buffer (10 mM Tris-HCl, 150 mM NaCl) and then developed using 0.03% hydrogen peroxide and 1 mg/ml 4-chloro-naphthol in 20% methanol for 5–15 min for optimal contrast. The reactivities of other monoclonal antibodies were tested in a similar fashion except that M2.4 and M2.6 were purified from ascites fluid and then diluted to a final concentration of 5–10 μg/ml in Tween buffer with BSA.

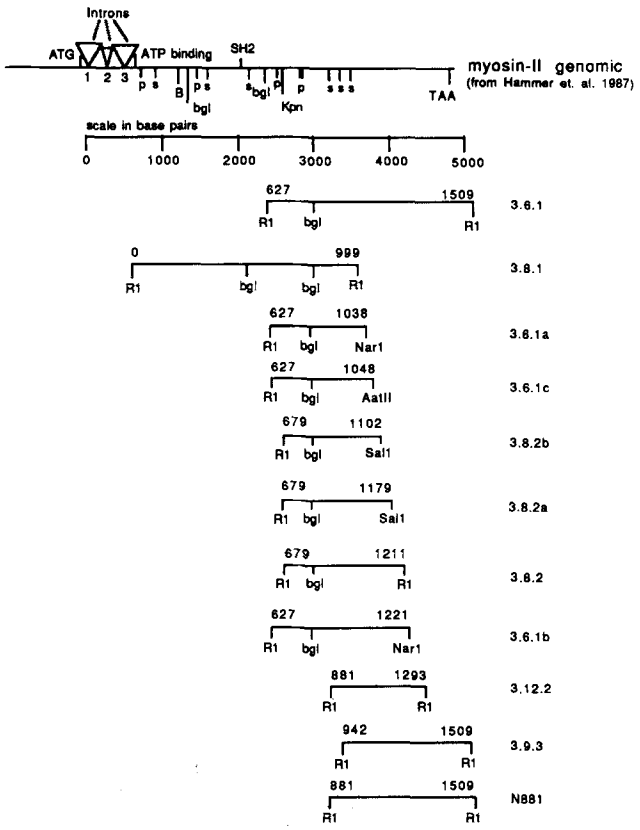

Figure 1. Restriction maps of cDNA clones and constructs purified and measured or used to localize the chemical binding sites of monoclonal antibodies. Restriction enzymes are indicated as follows: *P*, Pst; *S*, Sal; *B*, Bam HI; *bgl*, Bgl II; *RI*, Eco RI; other enzymes are shown without abbreviation.

Electron Microscopy and Data Analysis

Rotary shadowed molecules were prepared and viewed exactly as described in Kiehart et al. (1984*b*). Measurements were made using a lupe with a 100 μm grating on enlarged micrographs of the molecules. Measurements were made on all molecules in a given field regardless of their shape. Curved molecules were measured in multiple linear segments. Measurements were made from the head–tail junction to the center of mass of the antibody and to the tip of the tail. The head–tail junction was defined by the junction of a pear-shaped mass with a linear segment of substantially smaller diameter. There was no significant difference in the way the heads "fell" onto the grids nor was there any evidence that in some cases the heads fell in such a way to obscure the head–tail junction region. The microscope magnification was calibrated with paracrystals of skeletal muscle tropomyosin with a repeat of 39.5 nm.

Results

Overall Strategy

As noted in the introduction to this article, our first clue that there is a flaw in the standard model for myosin, with proline

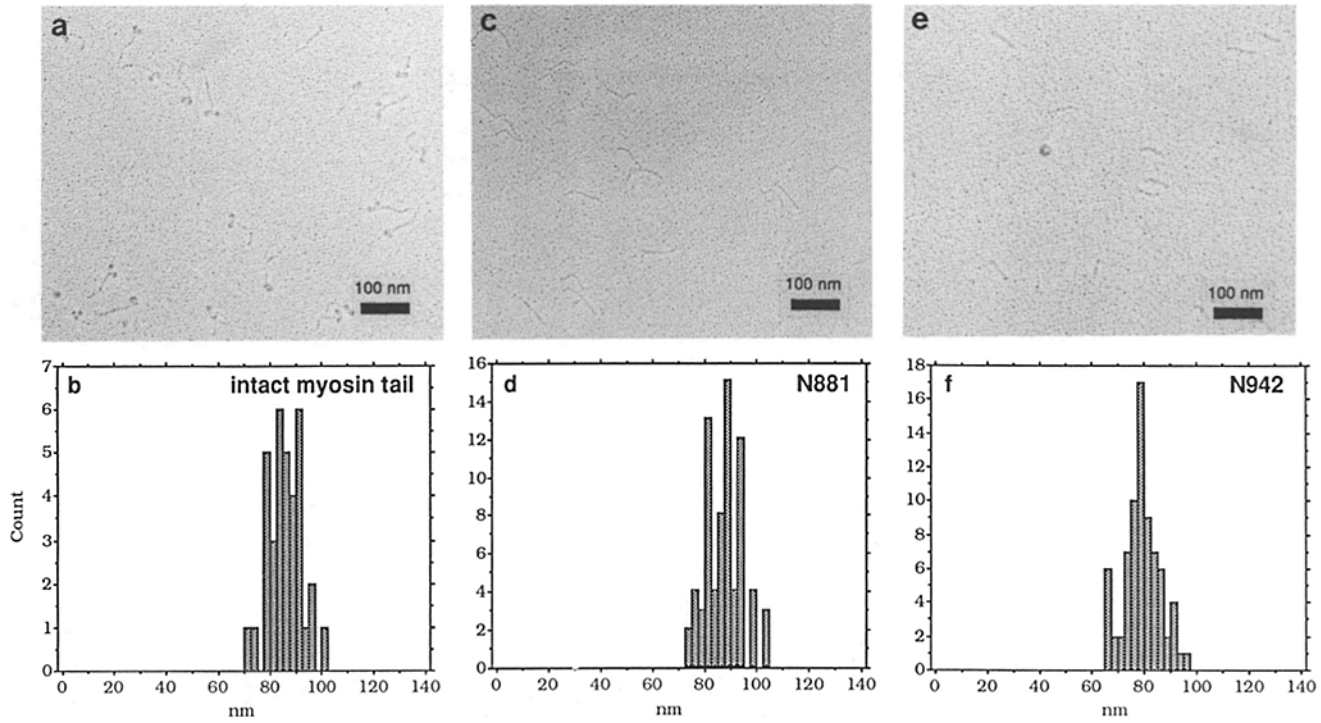

Figure 2. Electron micrographs of rotary shadowed replicas of purified myosin (*a*), and fusion proteins N881 (*c*) and N942 (*e*). Frequency distributions of measured lengths of the myosin-II tail (*b*) and fusion proteins N881 (*d*) and N942 (*f*). Means of the measured lengths are shown in Table 1.

847 at the head–tail junction, was the length of the tail of *Acanthamoeba* myosin-II. To investigate this discrepancy we have collected two complementary lines of evidence: the lengths of recombinant myosin tails composed of different numbers of amino acids and the correlation of the physical locations of seven monoclonal antibody binding sites and the regions of primary structure where these monoclonal antibodies bind. In the last section of Results we present an analysis of this data that supports a revised model for the myosin molecule.

Analysis of Shadowed Recombinant Myosin Tails

We compared electron microscopic images of native myosin-II with truncated myosin-II tails produced in *E. coli* from partial cDNA clones or constructs. As noted in previous studies (Pollard, 1982) rotary shadowed myosin-II consists of an extended tail with two heads at one end (Fig. 2 *a*). There is frequently a bend in the tail ~35 nm from the visible tip of the tail (Hammer et al., 1987). The tail has no other distinguishing features visible after rotary shadowing. The mean contour length (Fig. 2 *b*) of the myosin-II tail from the head–tail junction to the tip is 86.2 nm (SEM = 1.1 nm; SD = 6.5 nm) confirming previous measurements (Table I). Fusion protein N881 has 21 TrpE protein and linker amino acids at the NH_2 terminus followed by residues 881 to 1,509 of myosin-II. Fusion protein N942 is similar except that the 21 extra amino acids are followed by residues 942 to 1,509 of myosin-II. After shadowing (Fig. 2, *c* and *e*) these fusion proteins are identical in appearance except that N881 is longer (Fig. 2, *d* and *f* and Table I). Neither has recognizable structure at either end, showing that neither the 21 bacterial and linker amino acids at the NH_2 termini nor the 27 COOH-terminal amino acids (predicted to be nonhelical and not recognizable by rotary shadowing (Hammer et al., 1987)) are visible as distinct structures.

Physical and Chemical Locations of Monoclonal Antibody Binding Sites

We used electron microscopy to localize the binding sites for seven monoclonal antibodies. This work was begun by Kiehart et al. (1984*a*). We have reexamined a number of Kiehart's specimens and provide new data on antibody M2.46 (Fig. 3). Antibody M2.46 clearly binds the proximal tail a short distance away from the heat–tail junction. The other antibodies, M2.1, M2.4, M2.6, M2.10, and M2.22, all bind at sites that are indistinguishable from each other at the reso-

Table I. Comparison of Measured Contour Lengths with Theoretical Lengths

Molecule	Contour length	Theoretical length	Reference
	nm	*nm*	
Myosin-II tail	86.0	95.0	Pollard, 1982
Myosin-II tail	89.0	95.0	Kuznicki et al., 1985
Myosin-II tail	88.0	95.0	Hammer et al., 1987
Myosin-II tail	86.2	95.0	This work
N881 fusion	87.5	89.0	This work
N942 fusion	79.2	80.0	This work

Contour lengths were measured by election microscopy of shadowed myosin-II or recombinant fragments. The theoretical lengths were calculated assuming 0.148 nm/residue for the entire region of heptad repeats. The heptad repeats begin at residue 847 for myosin-II and at the NH_2 termini of the fusion proteins and end at residue 1,482. See the text for the rationale.

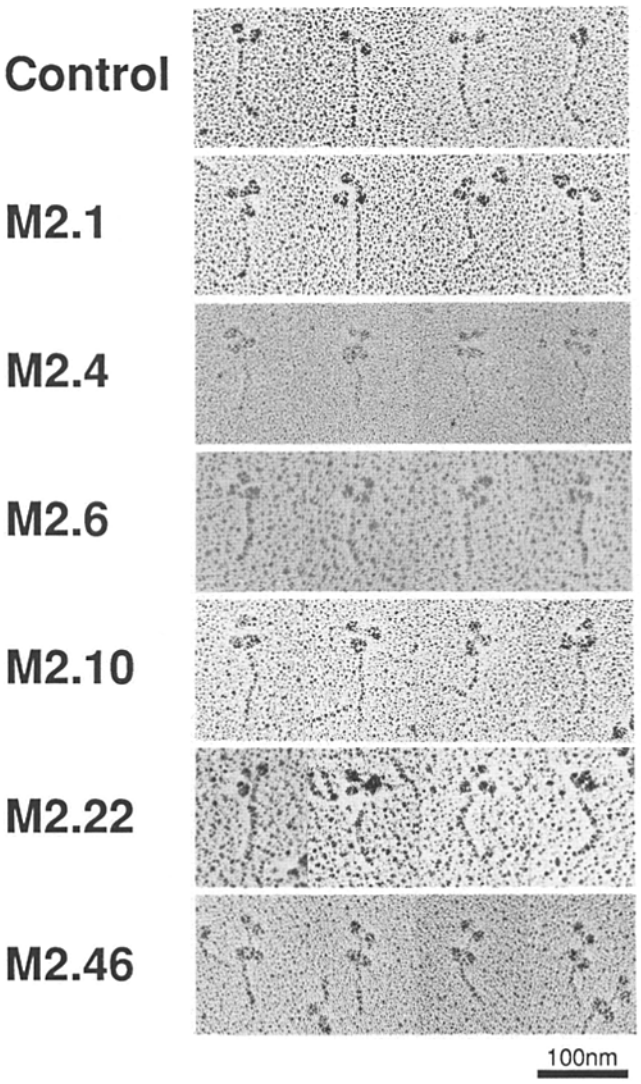

Figure 3. Localization of the binding sites for monoclonal antibodies to myosin-II by electron microscopy of rotary shadowed molecules. The monoclonal antibodies shown are M2.1, M2.4, M2.6, M2.10, M2.22, and M2.46. Undecorated myosin is shown as a control.

lution of the electron microscope. Some antibodies, for example M2.1, seem to bind between the two myosin heads as is seen in the leftmost example in Fig. 3. Others bind in a manner that makes them indistinguishable from the heads, as seen in the leftmost example of M2.4. We conclude only that they all bind near the head–tail junction. This is generally consistent with the conclusions drawn by Kiehart et al. (1984*a*) except for M2.4. They placed M2.4 19 nm down the tail from the head–tail junction. Our observations and new mapping data to be discussed later suggest that M2.4 is within 6 nm of the head–tail junction. This distance is just outside one standard deviation of Kiehart's measurement, a variation easily possible given the difficulty in measuring a 10–12-nm-wide structure and the difficulty in unambiguously distinguishing heads from antibody molecules.

We also mapped the chemical binding sites for all of these monoclonal antibodies along the polypeptide chain using a series of recombinant fusion proteins. This set represents segments of myosin-II cDNAs fused, in frame, to the TrpE protein in pATH vectors or to 12 amino acids of beta-galactosidase in pUCX vectors. They express proteins whose ends divide the myosin protein sequence into small increments. These expressed polypeptides were tested for ability to bind each monoclonal antibody on immunoblots. For example, M2.46 binds a fusion protein (3.8.2b) which ends at myosin-II residue 1,102 but does not bind another fusion protein (3.6.1a) which ends at residue 1048 (Fig. 4). We conclude that M2.46 binds to myosin-II between residues 1,048 and 1,102. Similarly we localized the binding sites for M2.1 and M2.22 between residues 942 and 999 and for M2.4, M2.6, and M2.10 between residues 881 and 942 (see Table II for summary). All of these antibodies appear to react with continuous epitopes since all bind to denatured myosin-II transferred to nitrocellulose after SDS-PAGE.

Calculation of the Amino Acid Sequence at the Head–Tail Junction

The first point we needed to establish is the length per residue in the myosin tail visualized by rotary shadowing. The theoretical rise per residue for alpha-helical coiled-coils, 0.1485 nm/residue (Fraser and Macrae, 1973), agrees very well with all the available electron microscopic data (Fig. 5). This value has been measured for tropomyosin (Phillips et al., 1986) and myosin tails (McLachlan, 1984). After rotary shadowing, our two headless tail fragments of known sequence fall precisely on the line with a slope of 0.148 nm/residue (Fig. 5). Similarly, the length of the *Dictyostelium* tail fragment "DdLMM-58" (DeLozanne et al., 1987) and the distance from the bend (presumed to be at proline 1,244 of *Acanthamoeba* myosin-II) to the end of the tail (Hammer et al., 1987) also fall exactly on the line with a slope of 0.148 nm/residue. We conclude that the rise per residue in myosin tails is 0.148 nm and that the number of amino acids can be measured accurately by electron microscopy of rotary shadowed molecules.

Using this calibration, the 86-nm tail of *Acanthamoeba* myosin-II consists of ~580 amino acids. The *Acanthamoeba* myosin-II consists of 1,509 amino acids as determined by translation of the nucleotide sequence of the gene (Hammer et al., 1987). Assuming that the tail ends at the COOH-terminal amino acid and is 100% helical, the head–tail junction would be at amino acid 929. However, Hammer et al. (1987) have argued convincingly that the 27 amino acids at the COOH terminus of the tail are not helical and unlikely to be visible in electron micrographs of rotary shadowed molecules. The lengths of our truncated fusion proteins and the distance from the kink to the tip of the tail are all consistent with this hypothesis. Therefore we assume that the visible tail ends at residue 1,482. This places the NH_2 terminus of the tail, the head–tail junction region, near residue 900.

Placement of the head–tail junction at residue 900 is further substantiated by the observation that the myosin-II tail is the same length as fragment N881 (Fig. 2). If the tail began at residue 847, this recombinant fragment would be 5 nm shorter than the native myosin tail. However we find that is ~1 nm longer. Our observation that fragment N942 is distinctly shorter, 79.2 nm (SEM = 0.8 nm; SD = 6.7 nm), establishes that a 6-nm size difference can be measured accurately by electron microscopy.

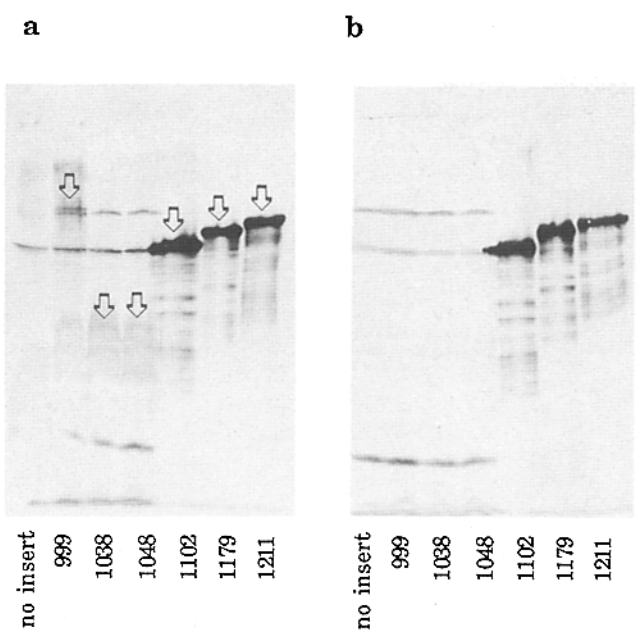

Figure 4. Localization of the chemical binding site for monoclonal antibody M2.46 between amino acids 1,048 and 1,102 by reaction with a panel of six different fusion proteins. Fusion proteins with COOH termini at residues 999–1,211, as indicated, were expressed in *E. coli*. Lysates were separated by gel electrophoresis in SDS, transferred to nitrocellulose and reacted with either (*a*) a mixture of monoclonal antibodies as a control to show the migration of the fusion proteins or (*b*) M2.46. The antibodies were detected with a peroxidase-labeled second antibody. Fusion proteins, shown by arrows in *a*, have the following molecular masses: 999 (113 kD); 1,038 (47 kD); 1,048 (48 kD); 1,102 (84 kD); 1,179 (93 kD); 1,211 (97 kD). Note that there is nonspecific staining of a number of bands or lysates without myosin-II inserts and detectable proteolysis of all of the fusion proteins.

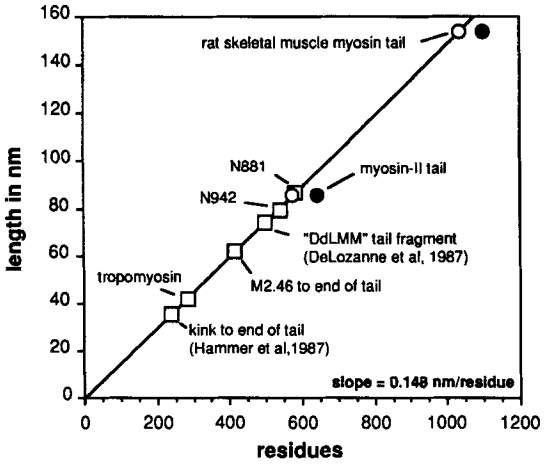

Figure 5. Rise per residue of coiled coil proteins. The relationship between the number of residues in an alpha-helix and its length measured by electron microscopy fits a model for myosin with the head–tail junction at residue 900. The standard curve is based on measured lengths of molecules with established sequences (□). The slope is 0.148 nm/residue. The circles show the measured lengths of two myosin tails. If the tails began at residue 900 (○), the length predicted from the number of heptad repeats falls precisely on the standard curve. If the tails began at residue 847 (●), the length predicted from the number of heptad repeats clearly falls off of the standard curve.

Our second argument for relocation of the head–tail junction at amino acid 900 is based on the location of monoclonal antibody M2.46. This antibody binds to myosin-II ~1/3 of the way down the tail. The physical distance from the antibody to the end of the tail (61.6 nm) agrees precisely with the number of residues (415) between the chemical binding site at ~1,070 and the end of the alpha-helical tail using 0.148 nm/residue (Figs. 5 and 6). On the other side, the physical distance between the head–tail junction and the M2.46 site (25 nm) is too small to accommodate the 230 residues between proline 847 and the antibody binding site at ~1,070 (Fig. 6). On the other hand these measurements are consistent with the head–tail junction located at residue 900.

A related line of evidence for the relocation of the head–tail junction is that all of the antibodies that bind near the head–tail junction have chemical binding sites around residue 940 rather than 847. Two of these antibodies (M2.1 and M2.22) bind in a region between amino acids 942 and 999. Three other monoclonal antibodies (M2.4, M2.6, and M2.10) compete with each other for binding and map chemically between amino acids 881 and 942 (Table II). Although the exact physical location of antibody binding sites near the head–tail junction is difficult to determine by electron microscopy due to the size of the antibody (10–12 nm), these results are clearly incompatible with the head–tail junction at residue 847. If that were true then M2.1 and M2.22 would bind 15–22 nm or 17–25% of the way down the alpha-helical tail. This distance, nearly twice the diameter of an antibody molecule, would be easily recognized and is clearly not seen in Fig. 3.

Table II. Epitope Mapping on Synthetic Fragments of Myosin-II

	Clone No./amino acids								
Antibody No.	3.12.2 881–1293	3.9.3 942–1509	3.8.1 1–999	3.6.1a 627–1,038	3.6.1c 627–1,048	3.8.2b 679–1,102	3.8.2a 679–1,179	3.8.2 679–1,211	Chemical binding site
M2.1	+	+	+	n	n	n	n	+	942–999
M2.4	+	0	+	n	n	n	n	+	881–942
M2.6	+	0	+	n	n	n	n	+	881–942
M2.10	+	0	+	n	n	n	n	+	881–942
M2.22	+	+	+	n	n	n	n	+	942–999
M2.46	+	+	0	0	0	+	+	+	1,048–1,102

A table showing which monoclonal antibodies bind to each clone. The numbers of the amino and carboxy terminus of each clone are shown. +, indicates binding; 0, indicates no binding; n, indicates not tested.

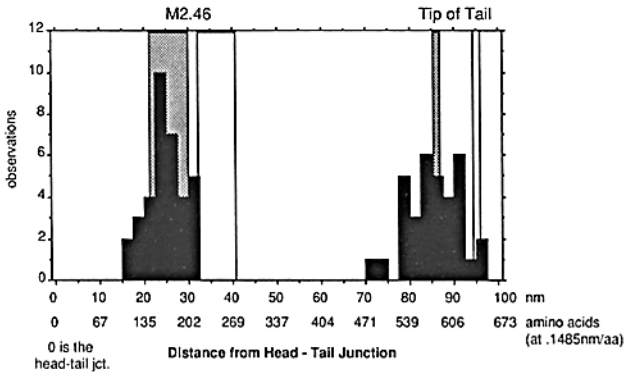

Figure 6. Comparison of the position of M2.46 binding measured by electron microscopy with the position of the chemical binding site between residues 1,048 and 1,102. The filled histograms show the distances from the head–tail junction to the center of mass of M2.46 and to the tip of the tail measured by electron microscopy. The shaded boxes show the location of the M2.46 antibody and the tip of the tail, as labeled, predicted by the new model with the head–tail junction at residue 900. The open boxes show the locations predicted by the old model with the head–tail junction at residue 847.

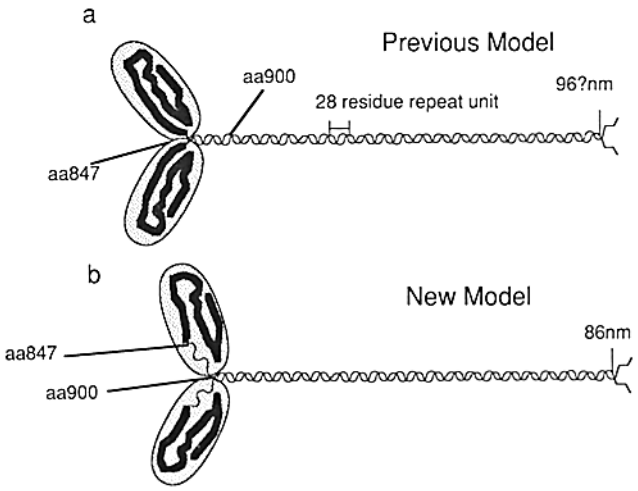

Figure 7. Drawing depicts (*a*) the old model where proline 847 is located at the head tail junction and (*b*) the new model with the head–tail junction at residue 900 and the first 8 heptad repeat units (~53 residues) within the head. According to this revised model, S-1 is cleaved from the tail domain by protease digestion within the head.

Our conclusions are summarized by the model shown in Fig. 7. We propose that ~53 amino acids, formerly assumed to be part of the tail, are physically part of the head. Although these sequences are predicted to be alpha-helical, we propose that they do not interact with each other to form a coiled-coil, but rather are independently located in the heads.

Discussion

The realization that the head–tail junction is at residue 900 in *Acanthamoeba* myosin-II suggests a new model for myosin (Fig. 7) with 53 residues of heptad repeat in the heads. Like other myosins, *Acanthamoeba* myosin-II has a strong heptad repeat starting at residue 847 (Hammer et al., 1987) which gives an alpha-helix an amphipathic character. In all known myosin sequences four of these heptad repeats form a 28-residue repeat unit with a strong band of positive charge followed by a band of negative charge 14 residues later (McLachlan, 1984). The side chains along one side of such a helix are almost entirely hydrophobic while the remaining surface is hydrophilic with alternating bands of positive and negative charges. In a coiled-coil the hydrophobic surfaces of the two amphipathic helices bind together while the alternating bands of positive and negative charges every 28 residues are available for ionic interactions between molecules that are required for filament formation. For the new model we assume that residues 847 to 900 are alpha-helical since the pattern of the sequence is not different in character from residues 900 to 1482. Instead of forming a coiled-coil, we suggest that the hydrophobic surface of the first 60 residues of helix binds to the surface of the head with the hydrophilic residues exposed to the solvent. There is no obvious break in the heptad repeat at residue 900, the proposed site for the head–tail junction. However detailed analysis of the myosin-II rod sequence has yet to be completed (Hammer, J. A., and A. D. McLachlan, manuscript in preparation).

We propose that the new model for *Acanthamoeba* myosin-II is applicable to other double headed myosins including muscle myosin. This proposal is supported by several different types of data. First, all known myosins have highly homologous head sequences extending from the NH_2 terminus to a proline near residue 847 (Warrick and Spudich, 1987). After this proline, the known myosin sequences are highly variable, but all exhibit a heptad repeat consistent with the formation of amphipathic alpha-helices such as those found in coiled-coils. These similarities in primary structure suggest that all myosins have essentially the same structure. For example, all known myosins can bind to any actin filament (Warrick and Spudich, 1987) and light chains can be exchanged between species (Kendrick-Jones et al., 1976). There are clearly some differences in details such as the presence of protease sensitive sites (Atkinson and Korn, 1986), but we expect the overall folding to be the same. Hence, conclusions about *Acanthamoeba* myosin-II should apply to other myosins.

Second, measured myosin tail lengths are consistent with the new model. Since longer myosin tails are more difficult to measure accurately than the short myosin-II tail, the discrepancy between length and primary structure has not been noted previously. The published values for the lengths of skeletal muscle myosin tails range from 137 nm (Lowey, 1969) to 154 nm (Stewart and Edwards, 1984). Elliott et al. (1976) observed that muscle myosin tail lengths from many species varied within 10 nm around 145 nm although he later (Elliott and Offer, 1978) reported the rabbit myosin tail is 156 ± 5 nm long. Although the amino acid sequence of the entire rabbit skeletal muscle myosin rod is not yet published, the tail length may be predicted from the highly homologous sequence of rat embryonic skeletal muscle myosin (Strehler et al., 1986) which has 1,101 residues between a proline at 838 and the COOH terminus, all compatible with a coiled-coil. A tail beginning at proline 838 would be 163 nm long, clearly greater than any mean length measured by electron microscopy. However with the head–tail junction at residue

900, the predicted length is 154 nm, in precise agreement with the longest values obtained by electron microscopy (Elliott and Offer, 1978; Stewart and Edwards, 1984; see Fig. 5).

Third, cleavage of S-1 from the tail of scallop muscle myosin seems to amputate the distal part of the head (Vibert, 1988). Based on the sequence of the COOH terminus of the cleaved heads, this cleavage is thought to occur just proximal to the invariant proline (Lu, 1980; Maita et al., 1987). The new model predicts that ~53 residues distal to the cleavage site would dissociate from the S-1 along with the tail, possibly accounting for the lost mass in the distal "neck" region of the isolated S-1 (Vibert, 1988). Previously this loss has been attributed largely to the dissociation of light chains.

Fourth, cleavage of scallop myosin with a lysine-specific protease (Winkelman et al., 1984) is also consistent with our new model. This protease leaves a nub consisting of the 20-kD COOH-terminal segment of S-1 attached to the tail. This nub is 10 ± 2 nm long and could easily contain both the 20-kD fragment of S1 as well as the first 53 amino acids of heptad repeat.

We expect that the 53 residues of heptad repeat, proposed to be physically part of the head, are bound rather loosely to S-1, since protease cleavage proximal to the invariant proline releases S-1 from tails under mild conditions. We cannot test this directly in *Acanthamoeba* myosin-II since the S-1 cleavage site is much less susceptible to proteolysis than a site 70 kD from the NH_2 terminus (Atkinson and Korn, 1986). A weakly bound segment of alpha-helix up to 9 nm long looks like an attractive hinge in the distal part of the heads, but the available evidence suggests that it may not be involved directly with the production of motion. The most convincing observations are the movement of actin filaments by S-1 in two in vitro assays (Toyoshima et al., 1987; Kishino and Yanagida, 1988).

In summary, we propose that the physical location of the head–tail junction as seen in electron micrographs is near amino acid 900 and that the proteolytic separation of S-1 from rod occurs within the myosin head.

We thank Dr. John Hammer III of the National Institutes of Health for providing the myosin-II genomic fragments used as probes to isolate cDNAs. Thanks also to Don Kaiser for antibody production and to Pam Maupin for assistance with electron microscopy.

This work was supported by National Institutes of Health research grant GM-26132 and a predoctoral fellowship to D. L. Rimm and J. H. Sinard from the Johns Hopkins School of Medicine Medical Scientist Training Program (GM07309).

Received for publication 29 October 1988 and in revised form 19 January 1989.

References

Atkinson, M. A. L., and E. D. Korn. 1986. The purification and characterization of a globular subfragment of *Acanthamoeba* myosin-II that is fully active when cross-linked to F-actin. *J. Biol. Chem.* 261:3382–3388.

Baker, T. A., A. D. Grossman, and C. A. Gross. 1984. A gene regulating the heat shock response in *Escherichia coli* also affects proteolysis. *Proc. Natl. Acad. Sci. USA.* 81:6779–6783.

DeLozanne, A., C. H. Berlot, L. A. Leinwand, and J. A. Spudich. 1987. Expression in *Escherichia coli* of a functional *Dictyostelium* myosin tail fragment. *J. Cell Biol.* 105:2999–3005.

Elliott, A., and G. Offer. 1978. Shape and flexibility of the myosin molecule. *J. Mol. Biol.* 123:505–519.

Elliott, A., G. Offer, and K. Burridge. 1976. Electron microscopy of myosin molecules from muscle and non-muscle sources. *Proc. R. Soc. Lond. B.* 193:45–53.

Elingza, M., and J. H. Collins. 1977. Amino acid sequence of a myosin fragment that contains SH-1, SH-2, and N-methylhistadine. *Proc. Natl. Acad. Sci. USA.* 74:4281–4284.

Emerson, C. P., and S. I. Bernstein. 1987. Molecular genetics of myosin. *Annu. Rev. Biochem.* 56:695–726.

Fraser, R. D. B., and T. P. Macrae. 1973. Conformation in Fibrous Proteins. Academic Press, Inc., New York.

Hammer, J. A., III, E. D. Korn, and B. M. Paterson. 1984. *Acanthamoeba* myosin IA, IB and II heavy chains are synthesized *in vitro* from *Acanthamoeba* messenger RNA. *J. Biol. Chem.* 259:11157–11159.

Hammer, J. A. III, B. Bowers, B. M. Paterson, and E. D. Korn. 1987. Complete nucleotide sequence and deduced polypeptide sequence of a nonmuscle myosin heavy chain gene from *Acanthamoeba*: evidence of a hinge in the rodlike tail. *J. Cell Biol.* 105:913–925.

Huynh, T. V., R. A. Young, and R. W. Davis. 1985. Constructing and screening cDNA libraries in λgt10 and λgt11. *In* DNA Cloning. Vol. 1: A Practical Approach. D. M. Glover, editor. IRL Press Ltd., Oxford, England. 49–78.

Karn, J. S., S. Brenner, and L. Barnett. 1983. Protein structural domains in *Caenorhabditis elegans* unc-54 myosin heavy chain gene are not separated by introns. *Proc. Natl. Acad. Sci. USA.* 80:4253–4257.

Kendrick-Jones, J., E. M. Szentkiralyi, and A. G. Szent-Gyorgyi. 1976. Regulatory light chains in myosins. *J. Mol. Biol.* 104:747–779.

Kiehart, D. P., D. A. Kaiser, and T. D. Pollard. 1984*a*. Direct localization of monoclonal antibodies binding sites on *Acanthamoeba* myosin-II and inhibition of filament formation by antibodies that bind to specific sites on the myosin-II tail. *J. Cell Biol.* 99:1015–1023.

Kiehart, D. P., D. A. Kaiser, and T. D. Pollard. 1984*b*. Monoclonal antibodies demonstrate limited structural homology between myosin isozymes from *Acanthamoeba*. *J. Cell Biol.* 99:1002–1014.

Kiehart, D. P., and T. D. Pollard. 1984*c*. Inhibition of *Acanthamoeba* actomyosin-II ATPase activity and mechanochemical function by specific monoclonal antibodies. *J. Cell Biol.* 99:1024–1033.

Kuznicki, J., G. P. Cote, B. Bowers, and E. D. Korn. 1985. Filament formation and actin-activated ATPase activity are abolished by proteolytic removal of a small peptide from the tip of the tail of the heavy chain of *Acanthamoeba* myosin-II. *J. Biol. Chem.* 260:1967–1972.

Laemmli, U. K. 1970. Cleavage of structural proteins during the assembly of the head of bacteriophage T4. *Nature (Lond.).* 227:680–685.

Lowey, S., H. S. Slayter, A. G. Weeds, and H. Baker. 1969. Substructure of the myosin molecule. *J. Mol. Biol.* 42:1–29.

Lu, R. C. 1980. Identification of a region susceptible to proteolysis in myosin subfragment-2. *Proc. Natl. Acad. Sci. USA.* 77:2010–2013.

Maita, T., M. Hayashida, Y. Tanioka, Y. Komine, and G. Matsuda. 1987. The primary structure of the myosin head. *Proc. Natl. Acad. Sci. USA.* 84: 416–420.

Maniatis, T., E. F. Fritch, and J. Sambrook. 1982. Molecular Cloning, A Laboratory Manual. Cold Spring Harbor Laboratory, Cold Spring Harbor, NY. 11 pp.

McLachlan, A. D. 1984. Structural implications of the myosin amino acid sequence. *Annu. Rev. Biophys. Bioeng.* 13:167–189.

McLachlan, A. D., and J. Karn. 1982. Periodic charge distributions in the myosin rod amino acid sequence match cross-bridge spacings in muscle. *Nature (Lond.).* 299:226–231.

Phillips Jr., G. N., J. P. Fillers, and C. Cohen. 1986. Tropomyosin crystal structure and muscle regulation. *J. Mol. Biol.* 192:111–131.

Pollard, T. D. 1982. Structure and polymerization of *Acanthamoeba* myosin-II filaments. *J. Cell. Biol.* 95:816–825.

Rimm, D. L., and T. D. Pollard. 1989. New plasmid vectors for high level synthesis of eukaryotic fusion proteins in *Escherichia coli*. *Gene.* In press.

Stewart, M., and P. Edwards. 1984. Length of myosin rod and its proteolytic fragments determined by electron microscopy. *FEBS (Fed. Eur. Biochem. Soc.) Lett.* 168:75–78.

Strehler, E. E., M. Strehler-Page, J. Perriard, M. Periasamy, and B. Nadal-Ginard. 1986. Complete nucleotide sequence and encoded amino acid sequence of a mammalian myosin heavy chain: evidence against intron-dependent evolution of the rod. *J. Mol. Biol.* 190:291–317.

Towbin, H., T. Staehelin, and J. Gordon. 1979. Electrophoretic transfer of proteins from polyacrylamide gels to nitrocellulose sheets: procedure and some applications. *Proc. Natl. Acad. Sci. USA.* 76:4350–4354.

Toyoshima, Y. Y., S. J. Kron, E. M. McNally, K. R. Niebling, C. Toyoshima, and J. A. Spudich. 1987. Myosin subfragment-1 is sufficient to move actin filaments *in vitro*. *Nature (Lond.).* 328:536–539.

Vibert, P. J. 1988. Domain structure of the myosin head in correlation averaged images of shadowed molecules. *J. Muscle Res. Cell Motil.* 9:147–155.

Warrick, H. M., and J. A. Spudich. 1987. Myosin structure and function in cell motility. *Annu. Rev. Cell Biol.* 3:379–421.

Warrick, H. M., A. DeLozanne, L. A. Leinwand, and J. A. Spudich. 1986. Conserved protein domains in a myosin heavy chain gene from *Dictyostelium discoideum*. *Proc. Natl. Acad. Sci. USA.* 83:9433–9437.

Winkelman, D. A., S. Almeda, P. Vibert, and C. Cohen. 1984. A new myosin fragment: visualization of the regulatory domain. *Nature (Lond.).* 307:758–760.